8-6-2005

Mathematical Model and Performance Analysis of a Liquid Desiccant Dehumidification Tower

Mark Alan Long

Recommended Citation

Long, Mark Alan, "Mathematical Model and Performance Analysis of a Liquid Desiccant Dehumidification Tower" (2005). *Theses and Dissertations*. 5304.
https://scholarsjunction.msstate.edu/td/5304

MATHEMATICAL MODEL AND PERFORMANCE ANALYSIS OF A

LIQUID DESICCANT DEHUMIDIFICATION TOWER

By

Mark Alan Long

A Thesis
Submitted to the Faculty of
Mississippi State University
in Partial Fulfillment of the Requirements
for the Degree of Master of Science
in Mechanical Engineering
in the Department of Mechanical Engineering

Mississippi State, Mississippi

August 2005

MATHEMATICAL MODEL AND PERFORMANCE ANALYSIS OF A

LIQUID DESICCANT DEHUMIDIFICATION TOWER

By

Mark Alan Long

Approved:

_____
Pedro Mago
Assistant Professor of Mechanical
Engineering
(Director of Thesis)

_____
B. Keith Hodge
Professor of Mechanical Engineering
(Committee Member)

_____
Louay M. Chamra
Associate Professor of Mechanical
Engineering
(Committee Member)

_____
Steven R. Daniewicz
Professor and Graduate Coordinator
of the Department of Mechanical
Engineering

_____
Kirk H. Schulz
Professor and Dean of the Bagley
College of Engineering

Name: Mark Alan Long

Date of Degree: August 6, 2005

Institution: Mississippi State University

Major Field: Mechanical Engineering

Major Professor: Dr. Pedro Mago

Title of Study: MATHEMATICAL MODEL AND PERFORMANCE ANALYSIS OF
                 A LIQUID DESICCANT DEHUMIDIFICATION TOWER

Pages in Study: 42

Candidate for Degree of Master of Science

A finite difference model simulating a liquid desiccant dehumidification tower with lithium chloride as the desiccant solution has been developed. The model determines the packing height needed for a condensation rate. Comparisons with experimental data illustrates that the model produces valid results. Air and desiccant solution temperatures within the dehumidification tower show that a temperature increase is experienced for both the air and desiccant solution from their respective entrances and exits from the tower. Increasing the air mass velocity or the amount of moisture removed from the air supply causes an increase in packing height. Increasing the desiccant mass velocity decreases the packing height.

DEDICATION

I would like to dedicate this research to my beloved daughter Tristen, my mother, June, my sister, Tracy Pitts, my grandmother, Hazel Blackwell, and to the memory of my grandfather Sammie Payne Blackwell.

ACKNOWLEDGEMENTS

TABLE OF CONTENTS

Page

Page

LIST OF TABLES

LIST OF FIGURES

NOMENCLATURE

a_t	total surface area density of packing (m^2/m^3)
a_w	wetted surface area of packing
C	constant pressure heat capacity (J/mol-K)
D	diffusivity (m^2/hr)
D_p	nominal size of packing (m)
F_G	gas mass transfer coefficient (mol/hr-m^2)
F_L	desiccant mass transfer coefficient (mol/hr-m^2)
G	gas mass velocity (mol/hr-m^2)
g	gravitational constant (m/hr^2)
H_G	enthalpy (J/mol)
h	heat transfer coefficient (J/hr-m^2-K)
J_D	Colburn j factor for mass transfer
J_H	Colburn j factor for heat transfer
$h_G{}'$	gas heat transfer coefficient corrected for mass transfer (J/hr-m^2-K)
k_G	gas mass transfer coefficient (mol/hr-m^2-Pa)
k_L	liquid mass transfer coefficient (m/hr)

L	liquid mass velocity (mol/hr-m^2)
M	molecular weight (g/mol)
P_B	partial pressure of dry air (Pa)
P_{Ai}	partial pressure of water vapor (Pa)
P_{lm}	logarithmic mean pressure difference defined by Eq. 16 (Pa)
Pr	Prandtl number
T	temperature (^{o}C)
U_S	percent liquid mass fraction (%)
X_S	liquid mass fraction (kg$_{LiCl}$/kg$_{solution}$)
x_A	liquid mole fraction (mol$_v$/mol$_{solution}$)
x_{Ai}	interfacial liquid mole fraction (mol$_v$/mol$_{solution}$)
x_{lm}	logarithmic mean liquid mole fraction difference (mol$_v$/mol$_{solution}$)
Y_A	gas mole ratio (mol$_v$/mol$_{dry\ air}$)
y_A	gas mole fraction (mol$_v$/mol$_{gas}$)
y_{Ai}	interfacial gas mole fraction (mol$_v$/mol$_{gas}$)
Z	packing height (m)

Greek:

λ	latent heat of condensation (J/mol)
μ	viscosity (kg/s-m)
ρ	density (kg/m^3)
σ	surface tension (N/m)

Subscripts:

A	water vapor
B	dry air
c	critical
i	interface
G	gas
L	liquid
o	reference state
S	desiccant solution

CHAPTER I

INTRODUCTION AND LITERATURE REVIEW

1.1 Introduction

The energy consumed in both residential and commercial buildings for space

conditioning in the United States accounts for 40 to 60% of the total energy consumption

of buildings [1]. In terms of cooling energy consumption for commercial buildings

alone, approximately 1.4 quads of primary energy are used annually in the U.S. [2]. Roth

et al. [3] presents a list of technological options related to HVAC systems that have the

potential to reduce energy consumption. These options include liquid desiccant air

conditioners, improved duct sealing, and variable refrigerant volume flow. Liquid

desiccant air conditioners, also referred to as hybrid liquid desiccant (HLD) cooling

systems, have the potential to reduce energy consumption for cooling and

dehumidification by handling the latent load independently from the sensible load. This

energy reduction can be as great as 0.2 quads with a payback period of 5 to 6 years [3].

A desiccant is a substance that has a high affinity for water, and can, be utilized to

extract moisture from the air. The desiccant is regenerated after becoming saturated with

moisture. Desiccants are classified as either liquid or solid. Examples of solid desiccants

include silica gel, activated alumina, lithium chloride salt, and molecular sieves. Liquid

desiccants include lithium chloride, lithium bromide, calcium chloride, and triethylene glycol solutions.

Commercial solid desiccant cooling systems are more readily available than are HLD cooling systems. Manufacturers such as Kathabar, Inc. and Niagara Blower Company do exist that provide liquid desiccant systems. However, this technology is still a relatively new technology for HVAC applications, but with continued research and development these systems can be commercialized within 3 to 4 years [3]. Research has shown that HLD cooling systems can be more cost effective than solid desiccant cooling systems. In terms of manufacturing cost, an HLD cooling system using a simple regenerator and a liquid desiccant that is evaporatively cooled costs approximately $0.60 per cubic foot per minute (cfm). A solid desiccant cooling system with a desiccant wheel and a rotary heat exchanger costs approximately $1.20 per cfm [3]. This is a manufacturing cost savings of about 50% for an HLD cooling system. Hybrid liquid desiccant cooling systems have the potential for operating costs 40% lower than for solid desiccant cooling systems. This cost savings is a result of liquid desiccants having a lower regeneration temperature and lower pressure drop and using the energy benefits of evaporative cooling [4]. Unlike a VCS, the liquid desiccant eliminates condensed moisture from collecting and providing an environment for harmful bacterial growth that can enter the air stream. Liquid desiccant have been found to capture air contaminants in air streams; therefore, a continuous supply of fresh air can be provided to a conditioned space. This will be very useful for hospitals where fresh air supply is very important for the well being of the occupants.

The main component of a solid desiccant system is the rotary wheel which has a porous matrix that contains the solid desiccant. The solid desiccant dehumidifies the air by adsorption. Adsorption involves the attraction of intermolecular forces between the molecules of the solid and the substance extracted from the gas. For dehumidification, a strong intermolecular force of attraction between the solid desiccant and the water vapor in the humid air exists. This attraction causes the water vapor to condense on the surface of the solid desiccant resulting in dehumidification of the air stream. The desiccant is regenerated by exposing the solid desiccant to a hot gas stream that increases the temperature of the water vapor on the surface. This causes the vapor pressure of the moisture to be greater than the hot gas stream, thus the moisture is transferred to the hot gas stream [5]. A schematic of a solid desiccant system is shown in Figure 1.1.
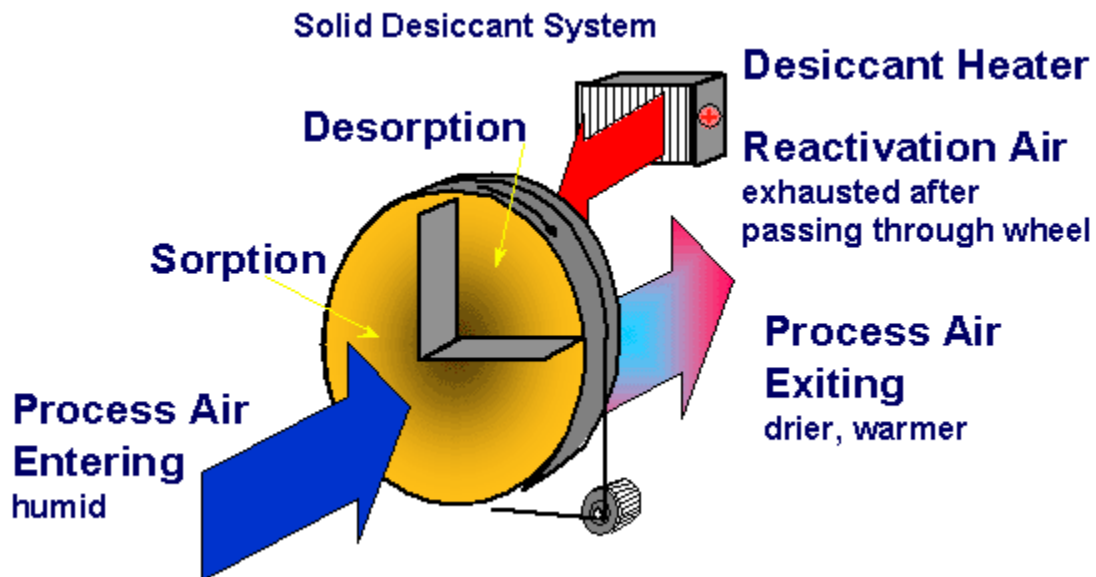
Figure 1.1 Solid Desiccant System Schematic
(http://www.eere.energy.gov/de/technologies/det_thermal_tech_basics.shtml)

The main components for a liquid desiccant system are the dehumidification and regeneration towers. As can be seen in Figure 1.2, moist air enters the bottom of the dehumidification tower and travels up through a packing material. The liquid desiccant enters the top of the tower and travels down the packing material countercurrent to the air. The packing material allows a large interfacial surface area to exist between the moist air and liquid desiccant to aid in mass transfer. The moist air entering the tower has a vapor pressure greater than the liquid desiccant. This causes the water vapor to be transferred from the air to the liquid desiccant, and dehumidified air leaves the tower. This type of mass transfer operation is known as absorption. The liquid desiccant becomes less concentrated after absorbing the water vapor from the moist air. The temperature of the weak desiccant is increased and enters the regeneration tower and travels down through the packing. The increase in temperature increases the desiccant vapor pressure. A supply of ambient air with a vapor pressure less than the desiccant flows countercurrently up through the regeneration tower and through the packing material. Water vapor is transferred from the desiccant to the ambient air due to the differences in vapor pressure.
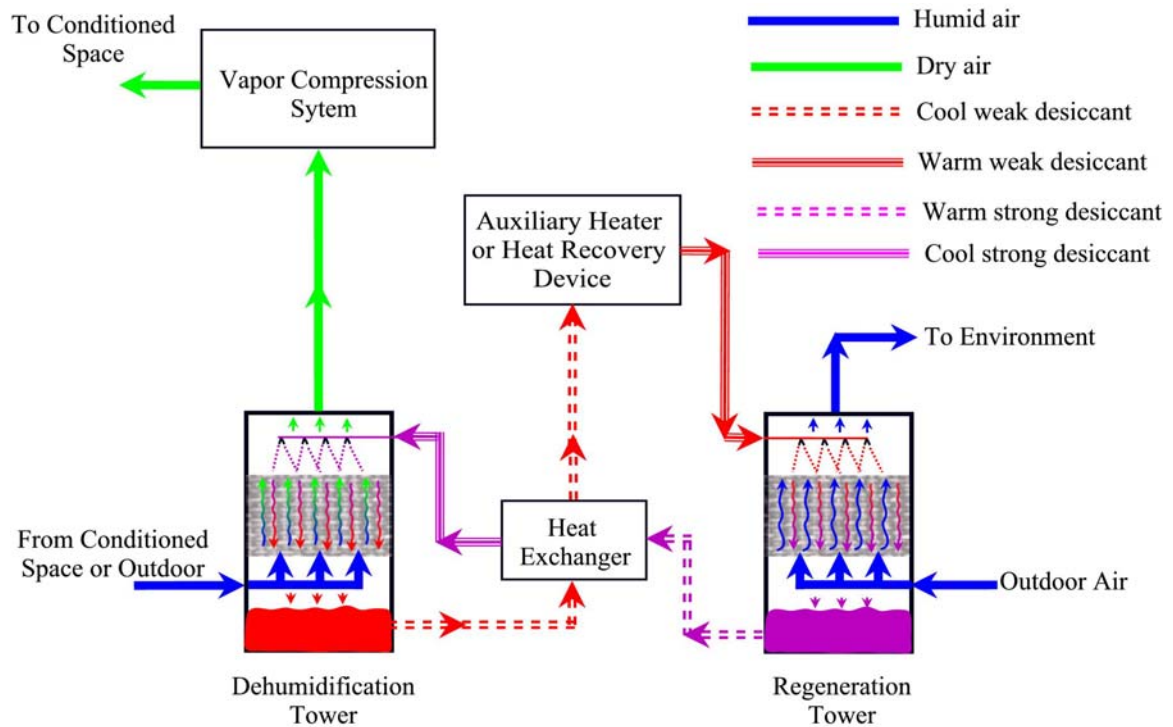
Figure 1.2 Hybrid Liquid Desiccant Cooling System

The objective of the present investigation is to develop a mathematical model to determine the packing height of a liquid desiccant dehumidification tower. Though the model developed in this research can be applied to any liquid desiccant, an aqueous LiCl solution was used to simulate the performance of the HLD cooling system in the model. The LiCl solution was chosen because it is a promising substance for commercial desiccant cooling applications.

1.2 Literature Review

The conventional air conditioning unit removes moisture from the air by lowering the temperature of the moist air below its dew point. The dehumidified air then is reheated to the desired comfort temperature for the conditioned space. This results in an inefficient process and can be improved by using a desiccant unit to handle the latent load independently from the sensible load. Figure 1.3 shows that the total change of enthalpy for a VCS, Δh_{VCS}, can be reduced if a HLD cooling system is used. This reduction can be attributed to the latent and sensible load being handled independently in a HLD cooling system. The dehumidification tower takes on the latent load ($h_1 - h_a$) while the evaporator would only handle the sensible load ($h_a - h_2$). Considering the energy consumption due to only cooling and dehumidifying the air, handling the latent and sensible load separately results in a significant reduction in energy consumption when compared to a VCS.
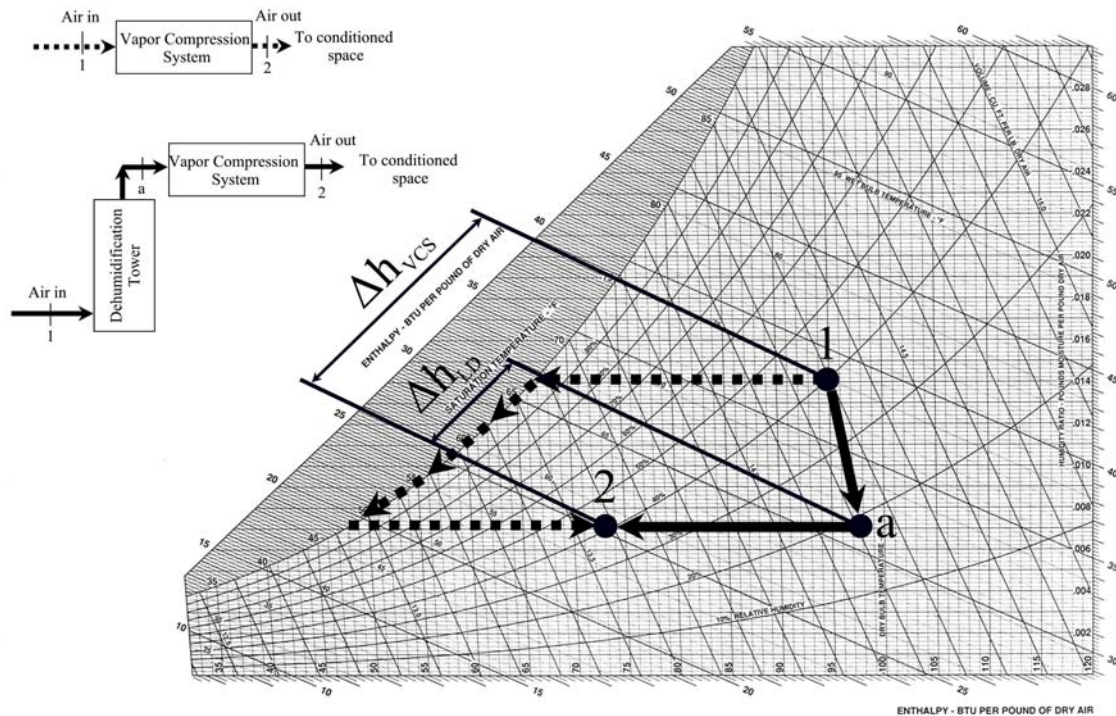
Figure 1.3 Cooling Paths for a Vapor Compression and HLD Cooling Systems

Various configurations of hybrid desiccant air conditioning systems have been studied. These systems have utilized either a solid or liquid desiccant to remove moisture from the conditioned air.

A field test house at the University of Florida was equipped with a hybrid liquid desiccant system [6]. Experiments were performed comparing the VCS and the HLD cooling system. The study determined that increases in airflow rate, inlet air temperature, or desiccant mass flow rate increased the rate of moisture removal, while increases in the inlet desiccant temperature decreased the rate of moisture removal.

At the University of Maryland, two cooling, heating, and power (CHP) systems were studied incorporating desiccant technology [7]. One CHP system used a solid desiccant and the other a liquid desiccant. The study was performed in order to compare

the two desiccant systems. The CHP system using the liquid desiccant did not produce electricity; however, waste heat from two engine-driven air conditioning units were recovered and used to regenerate the liquid desiccant. The CHP system using the solid liquid desiccant did produce electricity via a microturbine. The hot exhaust gases were recovered from the microturbine and used for heat generation in the absorption chiller and for regenerating the solid desiccant. The study found that the liquid desiccant unit consumed 9.5 kW of electrical power to produce 42 kW (12 tons) of cooling; whereas, a vapor compression system consumed 9.5 kW of electricity to produce 33 kW (9.4 tons) of cooling. The thermal coefficient of performance (COP) for the total cooling of the liquid desiccant system was found to be 1.0. The solid desiccant system removed more moisture from the air than the liquid desiccant system; however, due to the almost isenthalpic process after passing through the desiccant wheel the latent load is essentially converted to a sensible load. The thermal COPs for the total cooling for the solid desiccant system was 0.5. Both of the systems studied operated around 50% below design conditions. The COP for the systems could have been increased if operating conditions were at the design conditions. The two systems differed in these heat recovery methods; therefore, COP comparisons do not tell the complete story.

Similarly, a 20,000 m^2 demonstration building in Beijing, China was configured with a CHP system [8]. An internal combustion engine supplied power to the building with the waste heat used for an absorption chiller and for regeneration of a liquid desiccant system using lithium bromide as the desiccant. During peak electrical loads if the combustion engine could not supply the demand, then the power grid aided in

meeting the electrical demand. During peak thermal loads if waste heat could not supply the amount of energy needed to drive the absorption chiller, then a vapor compression unit was used to aid the absorption chiller. The regeneration of the liquid desiccant did not require any assistance during thermal peak hours due to the desiccants relatively low regeneration temperature. During the summer months, the CHP system continued to operate during the night and stored chilled water in a tank. The desiccant was also regenerated during the night, and the concentrated desiccant was placed in a storage tank. The potential thermal and chemical energy stored in these tanks was used during the peak thermal and electrical demand hours. During the winter months, the liquid desiccant system was used as a total heat exchanger to recover heat from the exhaust air. The CHP system was not used during the transition months, and the total electrical and thermal loads were handled by the power grid. Comparing to a conventional HVAC system, the CHP system was more energy efficient with the liquid desiccant system being an integral part of the increased efficiency. The payback period for the system was only 2 years.

A study performed in Beirut, Lebanon compared the feasibility for a liquid desiccant system using $CaCl_2$, for a low latent load building and a separate high latent load building [9]. The low and high latent load buildings were classified as residential and commercial, respectively. A residential liquid desiccant system was designed to completely replace the VCS and to handle the complete cooling load, latent and sensible. A liquid desiccant system was used in conjunction with a vapor compression unit in the restaurant, and is therefore, classified as a hybrid system. The COP for the residential building and the restaurant were found to be 0.41 and 0.45, respectively. Because the

latent and sensible load was handled separately, the size of the vapor compression unit for the restaurant was decreased from 11.4 to 8 tons of refrigeration. The hybrid system for the restaurant was found to be the most economically feasible, given a reasonable natural gas price for regenerating the liquid desiccant, and resulted in an immediate payback period if the liquid desiccant is regenerated with natural gas at a reasonable rate, and 11 years if a solar collector was used to assist the regeneration. Thus, a reduction in energy costs can be achieved by dehumidifying the air via a HLD cooling system for a building with a high latent load.

CHAPTER II

HEAT AND MASS TRANSFER INVESTIGATION

2.1 Two-Film Theory

As was mentioned earlier for a liquid desiccant dehumidification tower, moist air enters from the bottom and a concentrated liquid desiccant solution enters from the top of the tower. The mass transfer phenomena happens at the gas-liquid interface, as illustrated in Figure 2.1.   This figure shows that an average concentration exists in the bulk gas phase, y_A, and in the bulk liquid phase, x_A. As the bulk gas phase approaches the interface concentration, y_{Ai}, a thin laminar film, δ_G, develops and a decrease of the solute concentration of the gas phase exists. Across the interface, no mass transfer resistance is assumed exists; therefore, equilibrium concentrations are attained at the interface between the two phases at concentrations y_{Ai} and x_{Ai} for the gas and liquid phases, respectively. The solute is transferred to the liquid phase and also passes through a thin laminar film, δ_L, and the liquid concentration experiences a decrease in concentration from the interface to the bulk liquid. An interpretation of the mass transfer between the gas and liquid phase is known as the two-film theory and accounts for the resistances to mass transfer for the gas and the liquid phases.

Observing the concentration of the diffusing solute at the interface, the solute concentration seems to increase as the solute diffuses across the interface to the liquid phase. This is due to the use of different concentration units in the gas and liquid phase and does not represent a jump in concentration across the interface [5].
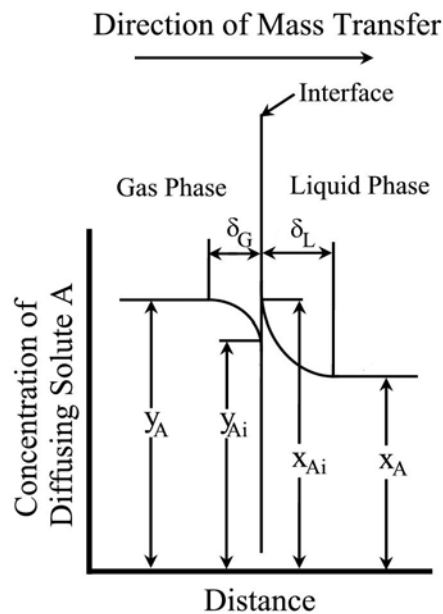
Figure 2.1 Two-Film Theory Diagram [5]

2.2 Heat Effects

Multiple heat effects can arise simultaneously in an absorption process. The heat of solution may increase the solvent temperature and decrease the equilibrium solubility of the solute. If a volatile solvent is used, for example, water, the vaporization of the solvent will absorb some of the sensible heat. The gas and liquid phases will experience sensible heat effects that are transferred to and from both phases. The heat effects

generated from the inside of the absorber will be transferred to the inside wall and then to the environment, unless cooling coils are incorporated in the absorber [10]. These effects of heat transfer in an absorption process can significantly alter the performance of the system. However, depending on the application one or all of the heat effects can be considered negligible to simplify performance calculations for the absorption process. Either isothermal or adiabatic processes are commonly assumed for performance calculations. The former being the most desired since the calculations are much simpler than the latter process. However, most absorption processes are exothermic for which temperature effects must be accounted [5]. Sawistowski and Smith [11] present a method to check whether isothermal or adiabatic conditions exist for performance calculations. Modeling the tower as an adiabatic process is a common assumption and has been shown to be accurate for large scale absorption towers [10]. This assumption is used in the development of the mathematical model which is described here in.

2.3 Model Development

A finite difference model was developed to determine the packing height of the dehumidification and regeneration towers. The procedure used in developing this model takes into account both the gas and liquid phase mass transfer resistances. This procedure is outlined and was first solved by Treybal [12]. There are cases where the resistance to mass transfer can be neglected and calculations can be simplified [13]. For example, in an air and pure water packed-tower configuration where the water is vaporized and absorbed by the air, the resistance to mass transfer exists entirely in the gas phase. However, for the case of an air and liquid desiccant packed-tower arrangement, at

the interface there exists a concentration gradient in the liquid and gas phases. Therefore,

both the gas and liquid phases must overcome a resistance for mass transfer to take place.

For solute concentrations greater than 40%, Löf et al. [14] state that the resistances to

heat and mass transfer in the liquid phase are small relative to the gas phase resistances

and can be neglected. The model constructed in this investigation accounts for the mass

transfer resistances for both the gas and liquid phases. There are assumptions

incorporated into the model in this thesis. These assumptions do not sacrifice any

accuracy from an engineering design perspective and are discussed in the following

paragraph.

The validity of the assumption of an adiabatic tower was discussed in Chapter 3

and was found to be acceptable for engineering purposes. The heat of solution is

assumed negligible. However, Sadasivam and Balakrishnan [15] state that neglecting the

heat of solution can result in an overdesign of the packing height. Data on the heat of

solution for LiCl solutions are available from Zaytsev and Aseyev [16] and can be

incorporated into the model. The scope of this thesis is concerned with preliminary

design calculations, and neglecting the heat of solution will give valid results for

engineering purposes. Another assumption used in the model is the interfacial surface

areas for the heat and mass transfer are equal. This assumption is stated because the

actual interfacial temperature is close to the value of the bulk liquid for liquid desiccant

absorption systems; therefore, the resistance to heat transfer for the liquid phase is

negligibly small relative to the heat transfer resistance in the gas phase. Axial dispersion

is assumed negligible and is considered to be minor [12] for any packed tower

application. In summary the assumptions are listed below:

1. The packed tower is adiabatic.

2. The heat of solution is neglected.

3. No resistance to heat transfer in the liquid phase; that is, the interfacial

    temperature is equal to the bulk liquid temperature.

4. The interfacial surface areas for heat and mass transfer are equal.

5. No axial dispersion; therefore, a one dimensional analysis is used.

Figure 2.2 displays the control volumes of a differential slice from the packed tower with

all significant material and heat effects entering and exiting the infinitesimal packing

height. The direction of mass and heat transfer is taken as positive from the gas to the

liquid.
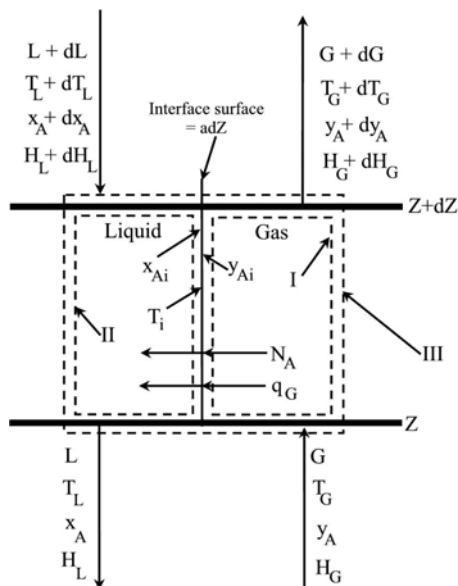
Figure 2.2 Differential Segment from a Packed Tower [12]

Incorporating the assumptions and the control volumes from Fig. 2.2, the equations that model the heat and mass transfer in the tower are listed below. The liquid side enthalpy can determined from

$$H_L = C_L(T_L - T_0) \tag{1}$$

Differentiating Eq. 1 we can write

$$dH_L = C_L dT_L \tag{2}$$

The gas-side enthalpy for low pressure can be expressed as

$$H_G = C_B(T_G - T_0) + Y_A[C_A(T_G - T_0) + \lambda] \tag{3}$$

Differentiating Equ. 3 we can write

$$dH_G = C_B dT_G + Y_A C_A dT_G + [C_A(T_G - T_0) + \lambda]dY_A \tag{4}$$

Evoking the conservation of mass principle across control volume III in Fig. 2.2 yields

$$dL = G_B dY \tag{5}$$

Performing an energy balance over control volume I, the heat transfer is given by

$$G_B H_G - G_B(H_G + dH_G) - (G_B dY)[C_A(T_G - T_0) + \lambda] = q_G a_t dZ \tag{6}$$

The heat transfer in Eq. 6 can be written as

$$q_G a_t dZ = h_G{}' a_t (T_G - T_L)dZ \tag{7}$$

Where the Ackerman correction for simultaneous heat and mass transfer is applied; that is

$$h_G{}' a_t = \frac{-G_B(C_A dY_A/dZ)}{1 - \exp[G_B(C_A dY_A/dZ)/h_G a_t]} \tag{8}$$

Combining Eqs. 4, 6, and 7 and rearranging, the change in gas temperature per change in differential packing height can be expressed as

$$\frac{dT_G}{dZ} = \frac{h_G{}'a_t(T_G - T_L)}{G_B(C_B + Y_A C_A)}$$

(9)

The change in gas solute concentration per differential height required for Eq. 8 is determined by writing the mass transfer for the gas, as is shown in Equation 10.

$$G_B dY_A = -F_G\left(\ln\frac{1-y_{Ai}}{1-y_A}\right)a_t dZ$$

(10)

Rearranging Eq. 10, the desired expression for the change in gas solute concentration per differential height is obtained.

$$\frac{dY_A}{dZ} = \frac{-F_G a_t}{G_B}\left(\ln\frac{1-y_{Ai}}{1-y_A}\right)$$

(11)

Evaluating Eq. 11 involves determining the equilibrium solute concentration at the interface as well as the gas-side mass transfer coefficient. A second order polynomial curvefit was formulated using vapor pressure data from Zaytsev and Aseyev [16] to determine the equilibrium mole fractions of the gas and liquid phases at the interface. This curvefit is expressed for the dehumidifier in Eq. 12.

$$y_{Ai} = \frac{4}{4053}\left[\begin{array}{l}(162 - 907T_L + 0.0184T_L{}^2) \\ + (-485 + 0.256T_L - 0.00509T_L{}^2)U_S \\ + (0.037 - 0.00176T_L + 0.00033T_L{}^2)U_S{}^2\end{array}\right]$$

(12)

Equation 12 is valid within the following temperature and percent concentration range:

$$25 \leq T_L \leq 70$$
$$20 \leq U_S \leq 40$$

The interfacial concentrations can also be expressed as

$$y_{Ai} = 1 - (1 - y_A)\left(\frac{x_A}{x_{Ai}}\right)^{F_L/F_G} \tag{13}$$

Equations 12 and 13 are solved simultaneously to determine the interfacial concentrations of the solute. The F-type mass transfer coefficients for the gas and liquid phase are computed from k-type coefficients from the following relationships.

For the gas:

$$F_G = k_G P_{lm} \tag{14}$$

For the liquid:

$$F_L = k_L x_{lm} \rho_L / M_L \tag{15}$$

where the logarithmic mean pressure difference, P_{lm}, in Eq. 14 is written as

$$P_{lm} = \frac{P_{Ai} - P_B}{\ln(P_{Ai}/P_B)} \tag{16}$$

Similarly for the logarithmic mean mole fraction difference, x_{lm}, in Eq. 15

$$x_{lm} = \frac{x_A - x_{Ai}}{\ln(x_A/x_{Ai})} \tag{16}$$

The k-type mass transfer coefficients and the wetted surface area, a_w, are calculated from the correlations developed by Onda, et al [17]. These correlations for the gas and liquid phase along with the correlation for the wetted surface area are shown in Equations 17-19, respectively.

$$k_G = 5.23 \frac{a_t D_G}{RT_G} \left(\frac{G}{a_t \mu_G} \right)^{0.7} \left(\frac{\mu_G}{\rho_G D_G} \right)^{1/3} \left(a_t D_p \right)^{-2.0} \tag{17}$$

$$k_L = 0.0051 \left(\frac{\mu_L g}{\rho_L} \right)^{1/3} \left(\frac{L}{a_w \mu_L} \right)^{2/3} \left(\frac{\mu_L}{\rho_L D_L} \right)^{-1/2} \left(a_t D_p \right) \tag{18}$$

$$\frac{a_w}{a_t} = 1 - \exp\left[-1.45 \left(\frac{\sigma_c}{\sigma} \right)^{0.75} \left(\frac{L}{a_t \mu_L} \right)^{0.1} \left(\frac{L^2 a_t}{\rho_L^2 g} \right)^{-0.05} \left(\frac{L^2}{\rho_L \sigma a_t} \right) \right] \tag{19}$$

The gas-phase heat transfer coefficient is determined from the heat and mass transfer analogy, which states that $J_D/J_H = 1$. Therefore:

$$h_G = F_G M_A \left(C_B + Y_A C_A \right) \frac{Sc^{2/3}}{Pr^{2/3}} \tag{20}$$

Performing a solute mass balance over control volume III in Fig. 2.2 gives

$$1 - \left(X_S + dX_S \right)\left(L + dL \right) + G_B Y_A = \left(1 - X_S \right)L + G_B \left(Y_A + dY \right) \tag{21}$$

Combining Eqs. 5 and 20, the change in desiccant concentration per segment height is expressed as

$$\frac{dX_S}{dZ} = -\frac{G_B X_S}{L} \frac{dY_A}{dZ} \tag{22}$$

The change in desiccant temperature per segment height is shown in Equation 23 and is

determined from an energy balance over control volume III in Fig. 2.2 and Eqs. 1, 2, 4,

and 5.

$$\frac{dT_L}{dZ} = \frac{G_B}{C_L L}\left\{(C_B + Y_A C_A)\frac{dT_G}{dZ} + [C_A(T_G - T_0) - C_L(T_L - T_0) + \lambda_0]\frac{dY_A}{dZ}\right\} \tag{23}$$

2.4 Solution Procedure

The finite difference model was written using the C++ computer language. Inputs

required for the program to execute are in the following list:

1. Humidity ratio

2. Inlet mass velocity of the gas

3. Inlet gas temperature

4. Inlet mass velocity of the liquid desiccant

5. Inlet liquid temperature

6. The amount of moisture to remove

7. The outlet gas temperature

8. The nominal size of the packing

9. The total surface area per volume of the packing

10. Number of segments into which the tower is divided

The inputs allow the conditions across the entire tower to be known except for the outlet

desiccant solution conditions. The outlet desiccant solution conditions are solved for;

thus, allowing all the boundary conditions across the entire tower to be known. The

tower is then divided into the number of segments entered into the model. Starting with

the first segment (at the bottom of the tower), the gas and liquid states for a segment are

determined. A comparison is then made between the calculated humidity ratio at the top

of the segment and the known humidity ratio at the top of the tower. If this comparison

shows that the humidity ratio at the top of the tower has not been reached, then another

segment is added, and the segment procedure is repeated until the required exit humidity

ratio is reached. The height of the segments to reach the exit humidity ratio determines

the required packing height for the tower. Flow charts delineating the procedure for

determining boundary conditions over the entire tower and the procedure for determining

gas/liquid states and height of each segment are presented in Figures 2.3 and 2.4,
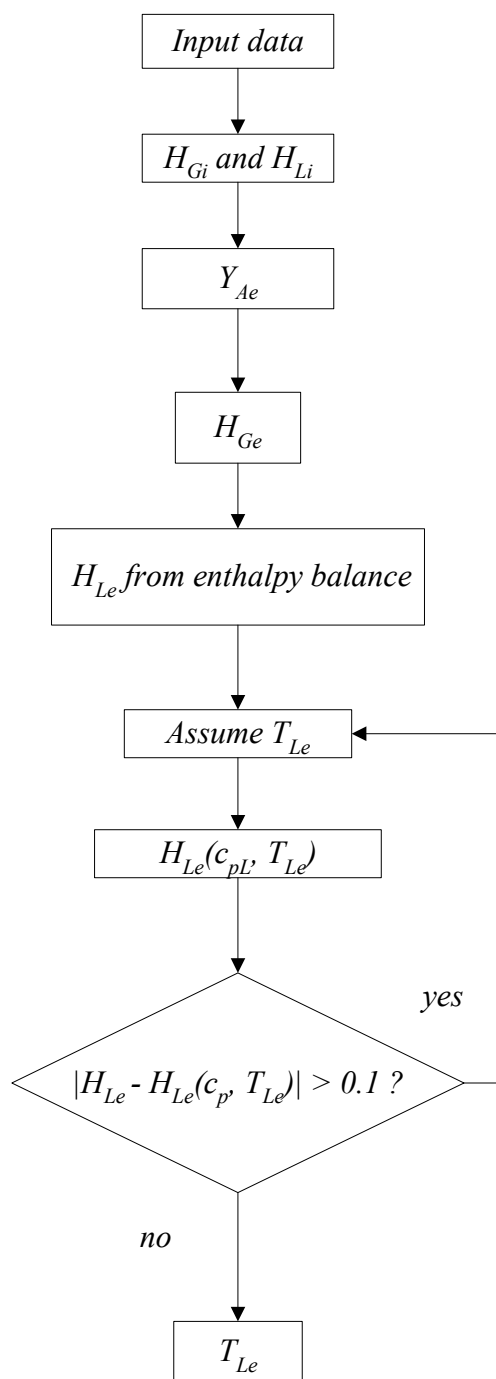
respectively.

Figure 2.3 Flow Chart for Determining all Gas/Liquid Inlet and Exit Conditions across the Entire Tower
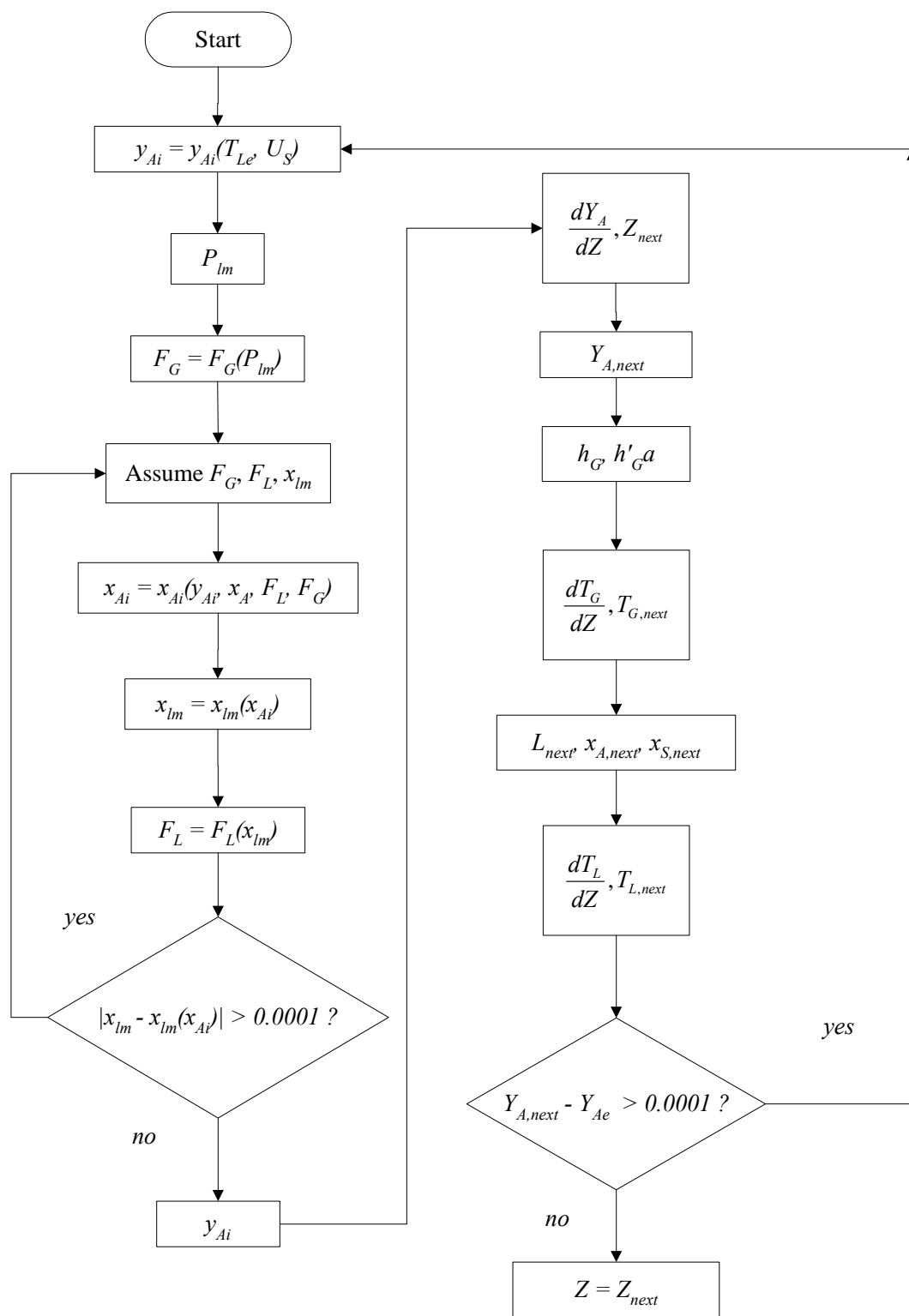
Figure 2.4 Flow Chart for Determining Segment Conditions and Packing Height

CHAPTER III

RESULTS AND DISCUSSION

3.1 Comparison with Experimental Data

The size and performance of a dehumidification tower was studied by simulating

varying operating conditions. The validity of the finite difference model was compared

with published experimental data reported by Fumo and Goswami [18] and Mago [19].

The desiccant solution used in both of the published works was aqueous LiCl. The

experimental setup was similar in both works being that inlet conditions entering the

tower were varied while the packing height remained at a constant value of 60 cm for

each experimental run. The packing size used in these works was 2.54-cm nominal

diameter and 210-m^2/m^3 specific surface area polypropylene Rauschert Hiflow$^®$ rings.

The method used for measuring the packing height was not discussed in Fumo and

Goswami or in Mago. Therefore, the accuracy of the height measurement is unknown.

Using their experimental data, the packing height was predicted using the finite

difference model (discussed in Chapter 2), with the tower divided into 100 segments.

The experimental data from Fumo and Goswami used for input in the model is presented

in Table 3.1, while the experimental data from Mago used for input in the model is

presented in Table 3.2. Comparisons between the simulated packing heights and the

actual packing heights from Fumo and Goswami are displayed in Figure 3.1,

while comparisons between the simulated packing heights and the actual packing heights from Mago are displayed in Figure 3.2. These figures illustrates that the finite difference model underpredicts the packing height for the majority of the experimental runs. The difference of magnitude between the actual and the predicted packing height is on the order of centimeters. Because the accuracy of the packing height measurement reported by Fumo and Goswami and Mago is unknown, the simulated height could be closer to the actual height that was reported from their experiments. However, from an engineering standpoint, the finite difference model produces acceptable results.

Table 3.1 Experimental Data from Fumo and Goswami [18]

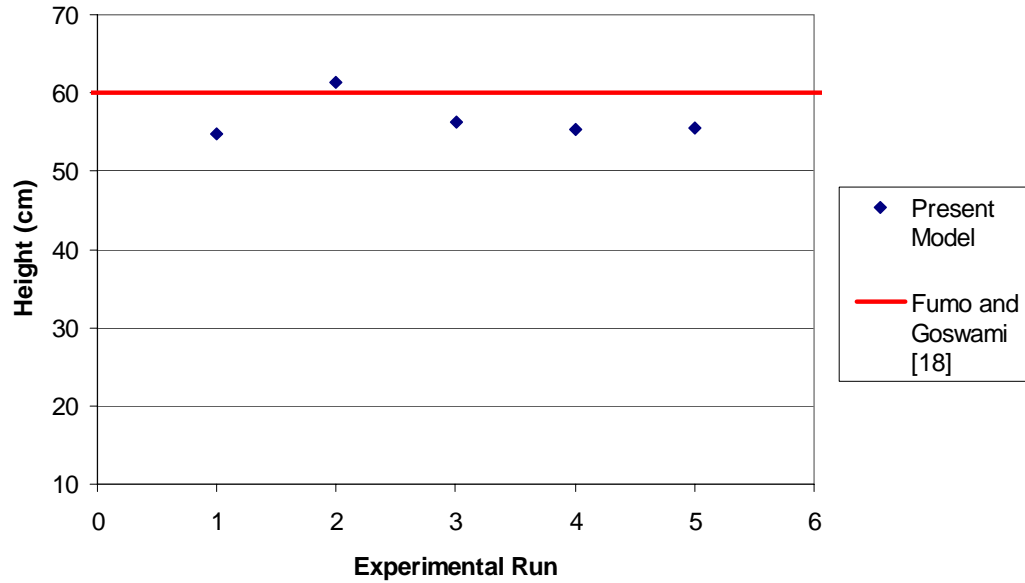| Inputs	Experimental Run				
	1	2	3	4	5
Humidity Ratio (kg_w/kg_{da})	0.0180	0.0181	0.0215	0.0181	0.0181
Gas Mass Velocity [$kg_{gas}/(s\text{-}m^2)$]	0.890	1.513	1.187	1.180	1.176
Inlet Gas Temperature (^oC)	30.1	30.2	29.9	30.1	30.0
Desiccant Concentration (kg_{LiCl}/kg_{sol})	0.346	0.343	0.339	0.347	0.348
Desiccant Mass Velocity [$kg_{sol}/(s\text{-}m^2)$]	6.124	6.113	6.272	6.227	6.206
Moisture to Remove (%)	42.22	40.33	44.19	40.33	40.88
Inlet Desiccant Temperature (^oC)	30.1	30.0	30.3	30.3	30.2
Outlet Gas Temperature (^oC)	31.3	32.2	33.4	32.2	32.0

Figure 3.1 Comparison of the Simulated Results with Fumo and Goswami [18]

Table 3.2 Experimental Data from Mago [19]

Inputs	Experimental Run		
	1	2	3
Humidity Ratio (kg_w/kg_{da})	0.0111	0.0111	0.0111
Gas Mass Velocity [$kg_{gas}/(s\text{-}m^2)$]	2.436	2.639	2.842
Inlet Gas Temperature (^{o}C)	26	26	26
Desiccant Concentration (kg_{LiCl}/kg_{sol})	0.35	0.35	0.35
Desiccant Mass Velocity [$kg_{sol}/(s\text{-}m^2)$]	2.084	2.084	2.084
Moisture to Remove (%)	18.02	19.82	18.92
Inlet Desiccant Temperature (^{o}C)	27	27	27
Outlet Gas Temperature (^{o}C)	27.6	26.7	27.6
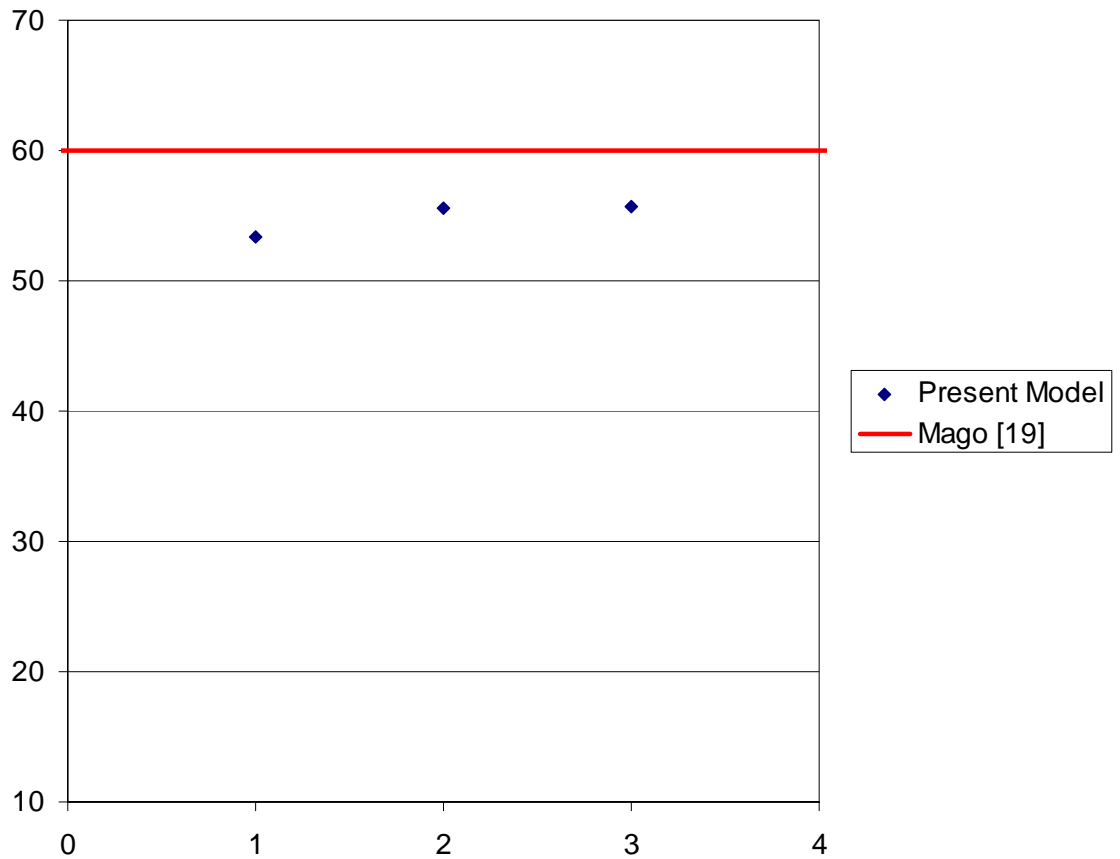
Figure 3.2 Comparison of the Simulated Results with Mago [19]

3.2 Performance Analysis

The finite difference model was used to simulate the performance of a liquid

desiccant dehumidification tower in a hot and humid climate with a dry bulb temperature

of 30.2 ^{o}C and relative humidity of 67%. The packing dimension used was the same as in

Fumo and Goswami's experiment. The temperature distribution within the tower (0

being the bottom of the tower) of the air and the liquid desiccant is presented in Figure

3.3. The data used to generate Figure 3.3 is displayed in Table 3.3.

Table 3.3   Simulation Input Used to Study the Temperature Distribution of the Air and
             Desiccant within the Dehumidification Tower

Humidity Ratio (kg_w/kg_{da})	0.0181
Gas Mass Velocity [$kg_{gas}/(s\text{-}m^2)$]	1.5
Inlet Gas Temperature (^{o}C)	30.2
Desiccant Concentration (kg_{LiCl}/kg_{sol})	0.35
Desiccant Mass Velocity [$kg_{sol}/(hr\text{-}m^2)$]	6
Moisture to Remove (%)	0.403
Inlet Desiccant Temperature (^{o}C)	30
Assumed Outlet Gas Temperature (^{o}C)	32

The temperature distribution of the air in Fig. 3.3 illustrates that the air

experiences an increase in temperature as the air enters the bottom of the tower and exits

at the top of the tower. Similarly, the desiccant also experiences an increase in

temperature as the desiccant enters the top of the tower and exits at the bottom. The

temperature trends for both the air and desiccant are expected since absorption is an

exothermic process; thus, the heat generated within the process increases the air and
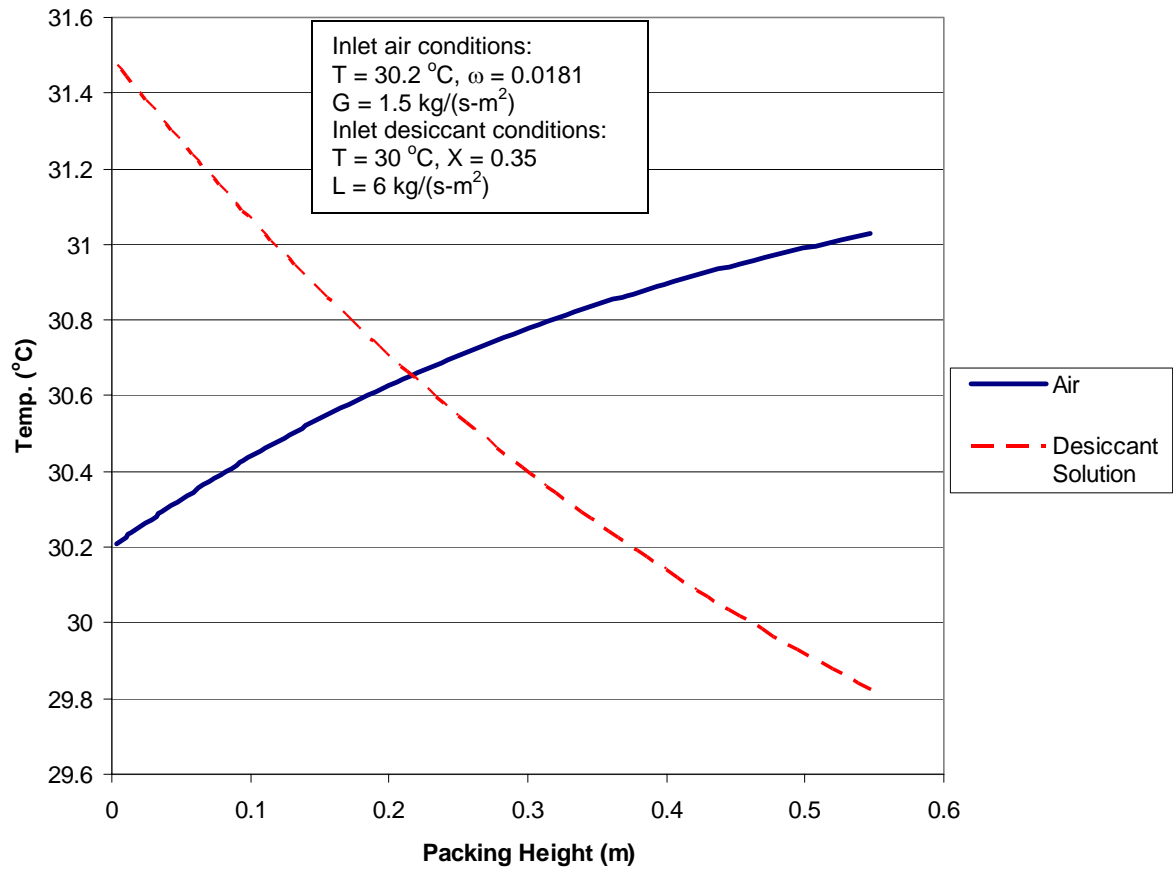
desiccant exiting temperatures.

Figure 3.3   Temperature Distribution of the Air and Desiccant Solution within the
               Dehumidification Tower

The outlet temperature of the air is an important property for a HLD cooling

system. The air leaving the tower enters the evaporator of a vapor compression system

for sensible cooling before entering the conditioned space. Therefore, the most energy

savings will result in having the lowest possible outlet temperature for the desired

moisture removal from the air. The variation of the outlet air temperature with the air

mass velocity and the inlet liquid desiccant temperature is presented in Figures 3.4 and

3.5. The data used to generate the results for these Figures are tabulated in Tables 3.4

and 3.5, respectively.

Table 3.4   Simulation Input Used to Study the Effect of the Air Mass Velocity on the
             Outlet Air Temperature

Humidity Ratio (kg_w/kg_{da})	0.0181
Gas Mass Velocity [kg_{gas}/(s-m^2)]	0.5 - 2
Inlet Gas Temperature (^{o}C)	30.2
Desiccant Concentration (kg_{LiCl}/kg_{sol})	0.35
Desiccant Mass Velocity [kg_{sol}/(hr-m^2)]	6
Moisture to Remove (%)	0.403
Inlet Desiccant Temperature (^{o}C)	30

Table 3.5   Simulation Input Used to Study the Effect of the Desiccant Inlet Temperature
             on the Outlet Air Temperature

Humidity Ratio (kg_w/kg_{da})	0.0181
Gas Mass Velocity [kg_{gas}/(s-m^2)]	1.5
Inlet Gas Temperature (^{o}C)	30.2
Desiccant Concentration (kg_{LiCl}/kg_{sol})	0.35
Desiccant Mass Velocity [kg_{sol}/(s-m^2)]	6
Moisture to Remove (%)	0.403

Figure 3.4 illustrates that increasing the air mass velocity will increase the outlet

air temperature. Figure 3.5 demonstrates that increasing the desiccant temperature

increases the outlet temperature. This trend in increasing outlet temperature with air

mass velocity and inlet desiccant temperature from Figs. 3.4 and 3.5 agrees with the

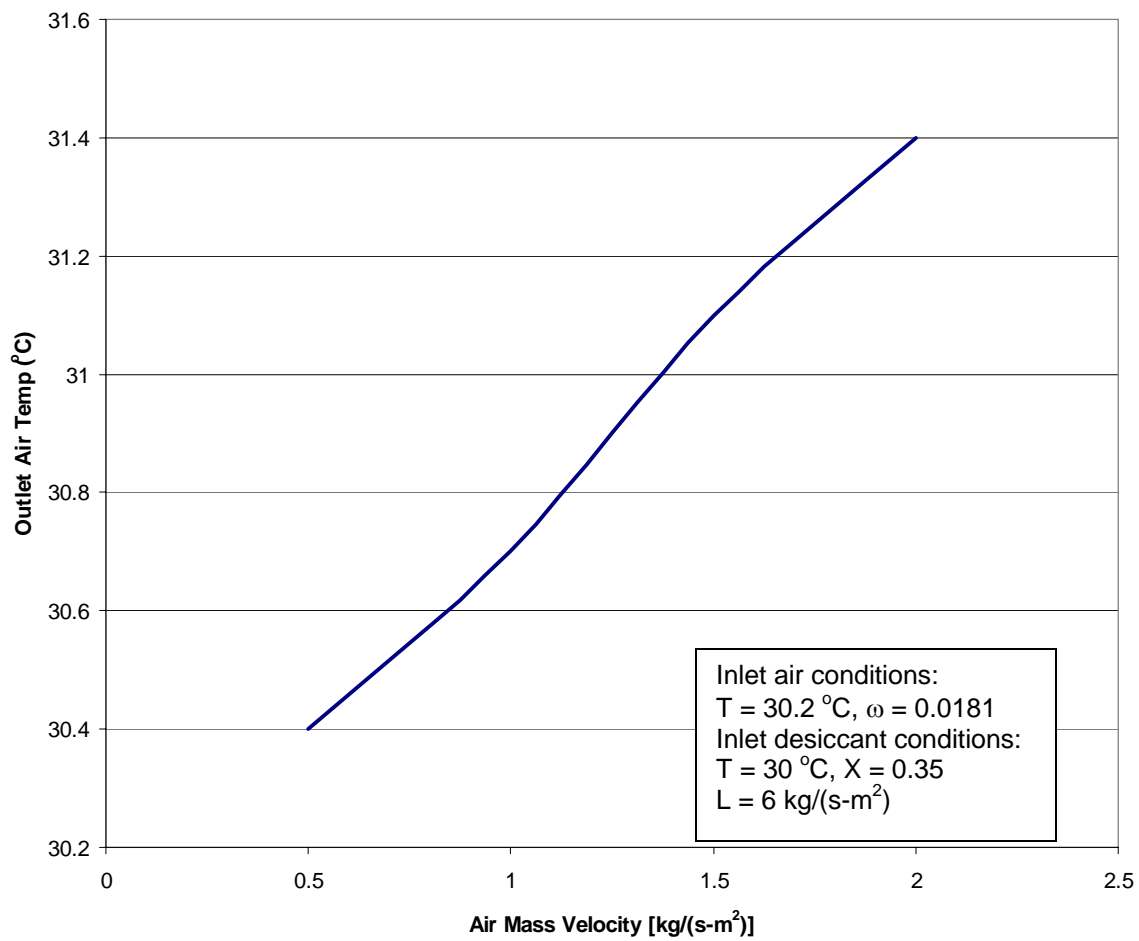experimental data of Mago and Goswami [6].

Figure 3.4 Outlet Air Temperature vs. Air Mass Velocity
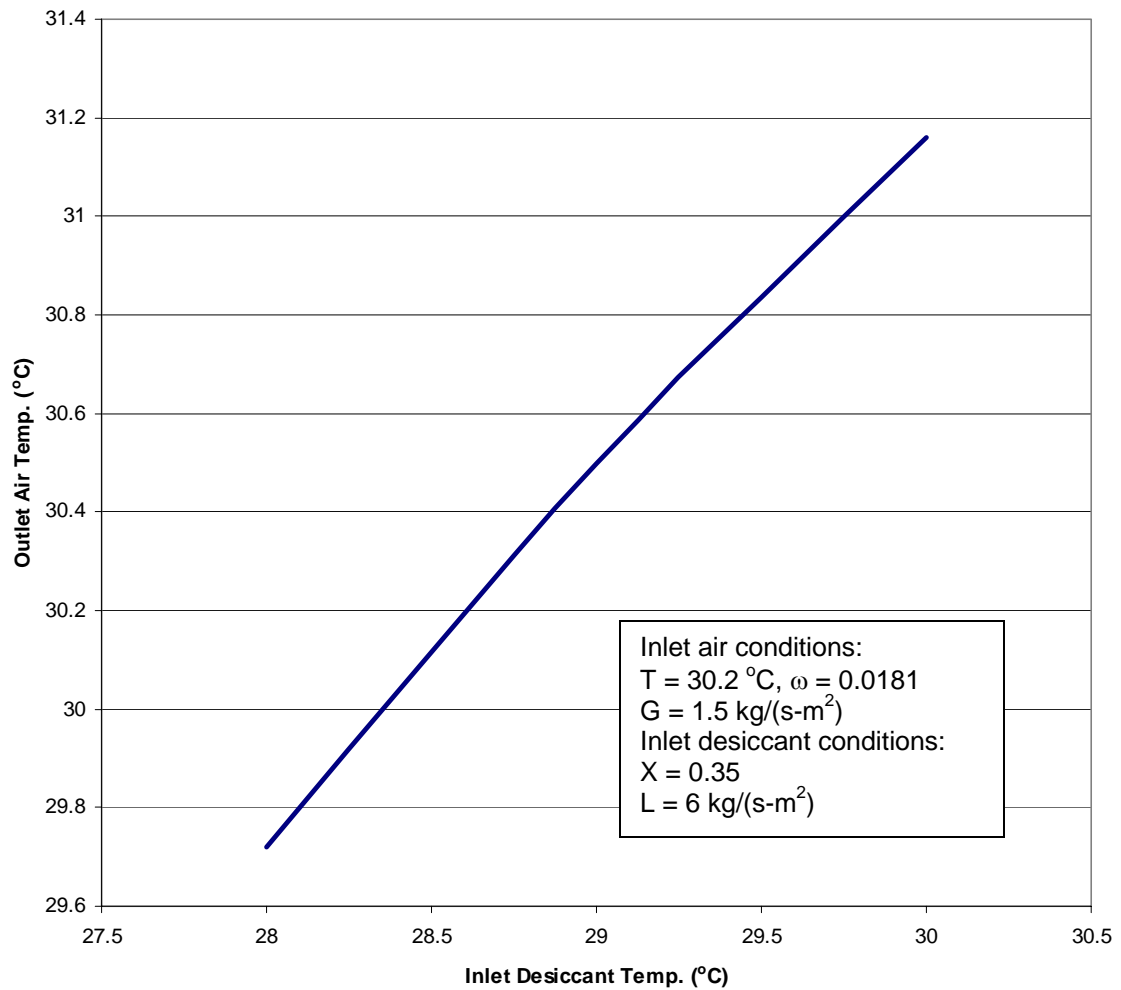
Figure 3.5 Outlet Air Temperature vs. Inlet Desiccant Temperature

3.3 Packing Height Analysis

The effects of the air mass velocity, desiccant mass velocity, and moisture

removed on the packing height for different desiccant are studied in this section. The

data used to study the effect of air mass velocity on packing height are presented in Table

3.6. Figure 3.6 demonstrates that increasing the air mass velocity results in an increase in

the packing height. This is because the air exposure time with the desiccant is decreased

as the flow rate increases. The packing height decreases as the desiccant concentration

increases. This results because the vapor pressure of the desiccant decreases with

increasing concentration, thus, increasing the mass transfer potential.

Table 3.6   Simulation Input Used to Study the Effect of the Air Mass Velocity on
Packing Height

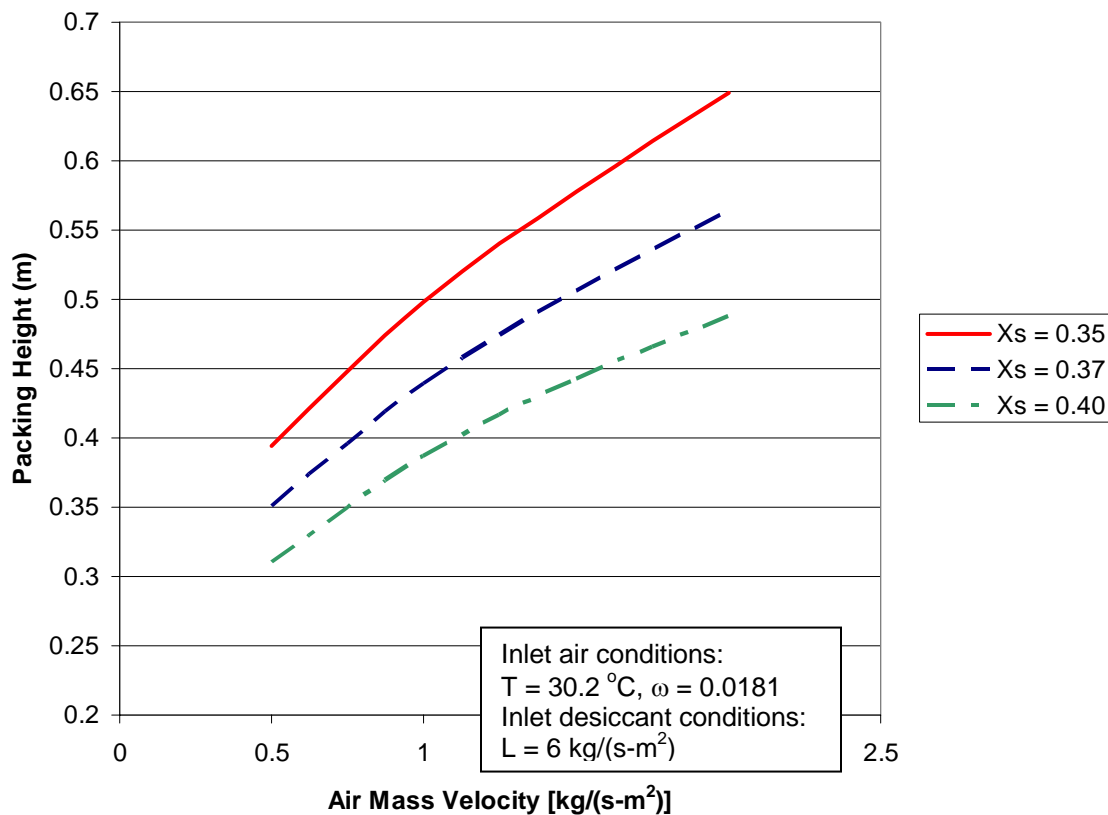|	
Humidity Ratio (kg_w/kg_{da})	0.0181
Inlet Gas Temperature (^{o}C)	30.2
Desiccant Mass Velocity [$kg_{sol}/(s\text{-}m^2)$]	6
Moisture to Remove (%)	0.403
Inlet Desiccant Temperature (^{o}C)	30
Assumed Outlet Gas Temperature (^{o}C)	32.2

Figure 3.6   Effect of Air Mass Velocity on Packing Height as Function of Liquid Mass Fraction

The data used to study the effect of effect of desiccant mass velocity on packing height are presented in Table 3.7, and the results are presented in Figure 3.7. This figure demonstrates that increasing the desiccant mass velocity and inlet concentration decreases the packing height. This is expected because increasing the desiccant flow rate allows more of the air to be exposed to a concentrated desiccant with the potential for mass transfer being increased. Increasing the desiccant concentration decreases the vapor pressure; therefore, the same effect of decreased packing height is illustrated in Fig. 3.7 as was in Fig. 3.6.

Table 3.7   Simulation Input Used to Study the Effect of Desiccant Mass Velocity on Packing Height

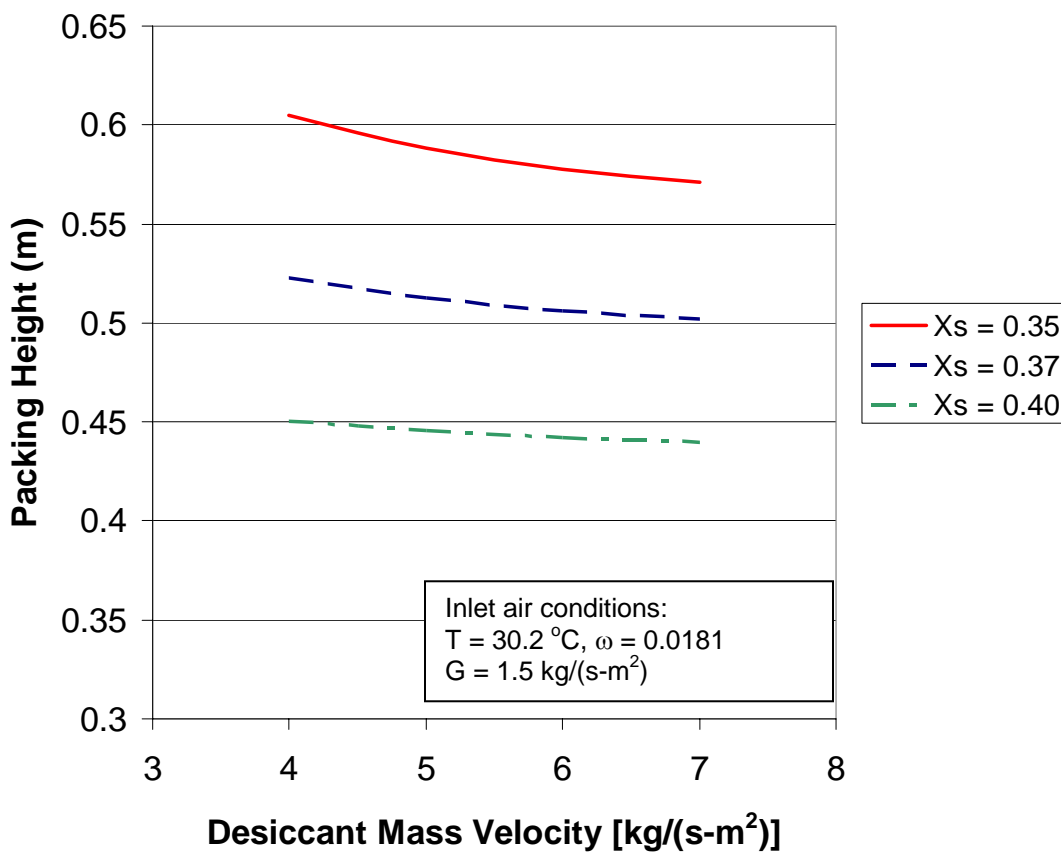| Humidity Ratio (kg_w/kg_{da})	0.0181
Gas Mass Velocity [$kg_{gas}/(s-m^2)$]	1.5
Inlet Gas Temperature (${}^oC$)	30.2
Desiccant Mass Velocity [$kg_{sol}/(s-m^2)$]	6
Moisture to Remove (%)	0.403
Assumed Outlet Gas Temperature (${}^oC$)	32.2

Figure 3.7   Effect of Desiccant Mass Velocity on Packing Height as a Function of Liquid Mass Fraction

The main objective of the dehumidification tower is to remove moisture from the air. Simulation data used to study the effect of moisture removed on packing height in shown in Table 3.8. Figure 3.8 shows that increasing the amount of moisture removed increases the mass transfer area; therefore, the tower height. The sharp increase in packing height as the moisture removal is increased demonstrates the sensitivity of tower performance to the amount of moisture that is removed from the inlet air.

Table 3.8   Simulation Input Used to Study the Effect of Moisture Removal on Packing Height

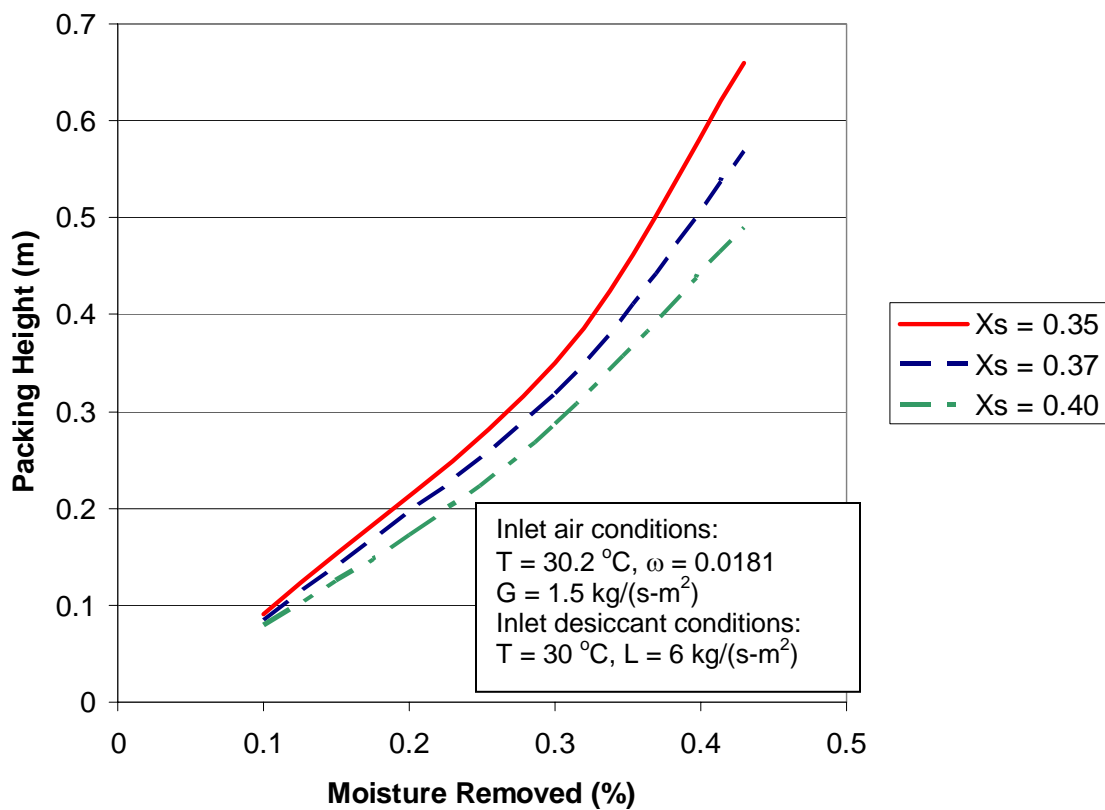|	
Humidity Ratio (kg_w/kg_{da})	0.0181
Gas Mass Velocity [kg_{gas}/(s-m^2)]	1.5
Inlet Gas Temperature (^{o}C)	30.2
Inlet Desiccant Temperature (^{o}C)	30
Desiccant Mass Velocity [kg_{sol}/(s-m^2)]	6
Assumed Outlet Gas Temperature (^{o}C)	32.2

Figure 3.8   Effect of Moisture Removed on Packing Height as a Function of Liquid
Mass Fraction

CHAPTER IV

CONCLUSIONS AND RECOMMENDATIONS

4.1 Conclusions

Energy consumption from a VCS can be reduced by handling the latent and sensible loads separately. A dehumidification tower using a liquid desiccant provides the means to remove the desired moisture from the air while the cooling coil in the VCS decreases the air temperature to the conditioned space. This handling of the latent and sensible loads independently allows the size of the VCS to be decreased when used in conjunction with a dehumidification tower, therefore, reducing equipment costs. An additional benefit provided by liquid desiccant technology is the ability to remove harmful contaminants from the supply air, which will be highly beneficial to hospitals because a supply of fresh air can be provided to the building. A liquid desiccant system is also beneficial for environments where the dew point temperature is below the freezing point of the moisture; thus, causing the cooling coil to become covered in ice which decreases the performance of the system. A Liquid desiccant dehumidifies the air on the principle of vapor pressure difference between the moist air and the liquid desiccant, therefore, eliminating ice formation on the cooling coil.

A finite difference model to simulate the height and performance of a packed tower was developed using the method by Treybal [12]. The packing height of a dehumidification tower was simulated using the finite difference model and the results were compared with experimental data [18, 19]. The analysis showed that the finite difference model results agreed well with the experimental data.

The performance of a dehumidification tower was analyzed by simulating a hot and humid climate. Results from the analysis demonstrated that the temperature distributions within the packed tower for the air and the liquid desiccant both experienced increases in temperature as the fluids traversed the tower. The outlet air temperature displayed an increase in value as the air mass velocity increased. Similarly, the outlet air temperature displayed an increasing trend as the inlet liquid desiccant temperature was increased.

The effects of air and liquid mass velocity, the amount of moisture removed, and desiccant concentration on the packing height of the tower were studied. The results illustrated that increasing the air mass velocity resulted in an increase in packing height. Increasing the desiccant mass velocity resulted in a decrease in packing height. Increasing the amount of moisture removal resulted in an increase in packing height. Increasing the desiccant concentration demonstrated a decrease in packing height.

4.2 Recommendations

Studies involving other liquid desiccant solutions can be applied to the finite difference model. These studies would allow performance and packing height comparisons. These comparisons can help determine the characteristics of the liquid desiccants for a given application.

Investigations involving an actual HLD cooling system experimental setup would allow operating and material cost to be analyzed. Methods using alternative energy sources could be implemented to study ways to regenerate the liquid desiccant and the costs associated with implementing the alternative energy sources on the system. The effect of the desiccant being entrained in the airflow and exiting the tower, known as carryover, can be studied and ways to eliminate it developed.

REFERENCES

[1]   "Heating and Cooling Systems,"
        http://www.eere.energy.gov/buildings/info/components/hvac/, March 15, 2005.

[2]   Westphalen, D. and Koszalinski, S., "Energy Consumption Characteristics of
        Commercial Building HVAC Systems Volume I: Chillers, Refrigerant
        Compressors and Heat Systems,"
        http://www.eere.energy.gov/buildings/info/documents/pdfs/hvacvolume1finalrepo
        rt.pdf, March 15, 2005.

[3]   Roth, K. W., Westphalen, D., Dieckmann, J., Hamilton, S. D., and Goetzler, W.,
        "Energy Consumption Characteristics of Commercial Building HVAC Systems
        Volume III: Energy Savings Potential,"
        http://www.eere.energy.gov/buildings/info/documents/pdfs/hvacvolume3finalrepo
        rt.pdf, March 15, 2005.

[4]   Lowenstein, A., Slayzak, S., Ryan, J., and Pesaran, A., "Advanced Commercial
        Liquid-Desiccant Technology Development Study,"
        http://www.nrel.gov/docs/fy99osti/24688.pdf, March 15, 2005.

[5]   Treybal, R. E., *Mass-Transfer Operations*. New York: McGraw-Hill Book
        Company, Inc., 1955.

[6]   Mago, P. and Goswami, D. Y., "A Study of the Performance of a Hybrid Liquid
        Desiccant Cooling System Using Lithium Chloride," *Journal of Solar Energy
        Engineering*, vol. 125, pp. 129-131, 2003.

[7]   Cowie, M., Xiaohong, L., and Reinhard, R., "Performance Comparison of Waste
        Heat-Driven Desiccant Systems," *Ashrae Transactions*, pp. 572-579, 2003.

[8]   Liu, X. H., Geng, K. C., Lin, B. R., and Jiang, Y., "Combined Cogeneration and
        Liquid-Desiccant System Applied in a Demonstration Building," *Energy and
        Buildings*, vol. 36, pp. 945-943, 2004.

[9]   Ghaddar, N., Ghali, K., and Najm, A., "Use of Desiccant Dehumidification to
        Improve Energy Utilization in Air-Conditioning Systems in Beirut," *International
        Journal of Energy Research*, vol. 27, pp. 1317-1338, 2003.

[10]   Stockar, U. v. and Wilke, C. R., "Rigorous and Short-Cut Design Calculations for Gas Absorption Involving Large Heat Effects. 1. A New Computational Method for Packed Gas Absorbers," *Industrial and Engineering Chemistry Fundamentals*, vol. 16, pp. 88-93, 1977.

[11]   Sawistowski, H. and Smith, W., *Mass Transfer Process Calculations*. New York: Interscience Publishers, 1963.

[12]   Treybal, R. E., "Adiabatic Gas Absorption and Stripping in Packed Towers," *Industrial and Engineering Chemistry*, vol. 61, pp. 36-41, 1969.

[13]   Sherwood, T. K. and Pigford, R. L., *Absorption and Extraction*. New York: McGraw-Hill Book Company, Inc., 1952.

[14]   Löf, G. O. G., Lenz, T. G., and Rao, S., "Coefficients of Heat and Mass Transfer in a Packed Bed Suitable for Solar Regeneration of Aqueous Lithium Chloride Solutions," *Journal of Solar Energy Engineering*, vol. 106, pp. 387-392, 1984.

[15]   Sadasivam, M. and Balakrishnan, A. R., "Analysis of Thermal Effects in Packed Bed Liquid Desiccant Dehumidifiers," *Chemical Engineering Process*, vol. 30, pp. 79-85, 1991.

[16]   Zaytsev, I. D. and Aseyev, G. G., *Properties of Aqueous Solutions of Electrolytes*: CRC Press, 1992.

[17]   Onda, K., Takeuchi, H., and Okumoto, Y., "Mass Transfer Coefficients Between Gas and Liquid Phases in Packed Columns," *Journal of Chemical Engineering of Japan*, vol. 1, pp. 56-62, 1968.

[18]   Fumo, N. and Goswami, D. Y., "Study of an Aqueous Lithium Chloride Desiccant System: Air Dehumidification and Desiccant Regeneration," *Solar Energy*, vol. 72, pp. 351-361, 2002.

[19]   Mago, P., "Performance of a Hybrid Desiccant Cooling System Using Lithium Chloride and its Application in Residential and Commercial Sector," in *Mechanical and Aerospace Engineering*, Masters Thesis: University of Florida, 2000.